



The role of the interface structure on the growth of nonpolar (10 $\bar{1}$ 0) and semipolar (11 $\bar{2}$ $\bar{2}$) ZnO on (112) LaAlO $_3$ substrates



Jr-Sheng Tian, Yue-Han Wu, Wei-Lin Wang, Tzu-Chun Yen, Yen-Teng Ho, Li Chang*

Department of Materials Science and Engineering, National Chiao Tung University, Hsinchu, Taiwan

ARTICLE INFO

Article history:

Received 7 June 2013

Accepted 19 June 2013

Available online 26 July 2013

Keywords:

Structural

Epitaxial growth

Interfaces

LaAlO $_3$

ZnO

ABSTRACT

Growth of nonpolar (10 $\bar{1}$ 0) and semipolar (11 $\bar{2}$ $\bar{2}$) ZnO on (112) LaAlO $_3$ (LAO) substrates can be obtained by annealing the substrate surface in vacuum and oxygen ambient conditions prior to ZnO deposition, respectively. We investigated the origin of the two different growth relationships by inspecting their interface in atomic scale using high angle annular dark field scanning transmission electron microscopy. (10 $\bar{1}$ 0) ZnO was grown on flat (112)_{LAO} surface due to the similar atomic configurations and small lattice mismatch between them at the interface, and (11 $\bar{2}$ $\bar{2}$) ZnO was grown on a faceted surface with (001)_{LAO} and (110)_{LAO} facets on which accommodation growth of both (11 $\bar{2}$ 0) ZnO and (000 $\bar{1}$) ZnO are consistent with [1 $\bar{1}$ 00]_{ZnO}//[1 $\bar{1}$ 0]_{LAO}.

© 2013 Elsevier B.V. All rights reserved.

1. Introduction

Wurtzite zinc oxide (ZnO), a non-toxic, transparent and wide-direct bandgap semiconductor, is promising for optoelectronic applications due to the large exciton binding energy (60 meV) [1]. Since wurtzite structure has no inversion center, polarization could cause detrimental effect on the luminescent properties [2,3]. To reduce such an effect, wurtzite materials grown along nonpolar and semipolar orientations have been intensively studied [4,5]. Owing to the lack of large size and cheap ZnO substrates, growth of nonpolar and semipolar ZnO is usually carried out on foreign substrates [6–9].

LaAlO $_3$ (LAO), a perovskite structure which is R $\bar{3}c$ (trigonal lattice) at room temperature and Pm $\bar{3}m$ (cubic lattice) at temperature above 540 °C, has been used as substrate to grow various oriented ZnO. For simplicity, R $\bar{3}c$ LAO can be treated as pseudo-cubic with lattice parameter of 3.791 Å. Recently, we have demonstrated the growth of nonpolar (11 $\bar{2}$ 0), (10 $\bar{1}$ 0), and (1340) oriented ZnO on (001), (112), and (114) LAO substrates, respectively [7,10,11]. Also, semipolar (11 $\bar{2}$ $\bar{2}$) ZnO can be deposited on LAO-buffered (112) (LaAlO $_3$) $_{0.29}$ (Sr $_2$ AlTaO $_6$) $_{0.35}$ (LSAT) substrate [12]. These results represent that the structure and chemistry of LAO substrates are favorable for achieving epitaxial ZnO films. However, it is of interest to find out why ZnO growth on (112) LAO substrate exhibits a different orientation from that on (112) LAO/LSAT.

In this report, we first show that (11 $\bar{2}$ $\bar{2}$) ZnO can also be obtained on (112) LAO substrates by adopting the same condition as for the

growth of (11 $\bar{2}$ $\bar{2}$) ZnO on (112) LAO/LSAT [12]. Next, we investigate the interface structures of nonpolar (10 $\bar{1}$ 0) and semipolar (11 $\bar{2}$ $\bar{2}$) ZnO on LAO substrates with their epitaxial relationships.

2. Experimental

ZnO films were grown by pulsed laser deposition using a KrF excimer laser. A laser fluence of ~ 3 J/cm 2 on a sintered ZnO target and 99.999% oxygen as ambient gas were adopted for the growth. Prior to ZnO deposition, (112) LAO substrates were annealed at two different ambient conditions, vacuum and oxygen pressure of 100 mTorr, both at 850 °C for 1 h. All the deposited ZnO films were then grown in the same condition at 750 °C and 50 mTorr for 30 min with pulse rate of 5 Hz.

Growth orientations of the ZnO films were investigated by using X-ray diffraction (XRD) (Cu K $_{\alpha 1}$). The interface structures of ZnO/LAO were studied by using high angle annular dark field (HAADF) scanning transmission electron microscopy (STEM) to reveal the Z-contrast due to the difference in atomic number. The HAADF images were acquired in a JEOL ARM 200F microscope which provides STEM image resolution of 0.08 nm. The STEM specimens were prepared by a conventional method consisting of mechanical grinding and ion milling.

3. Results and discussion

XRD patterns in Fig. 1 show that the growth orientation of the ZnO film on (112) LAO substrates with vacuum annealing is in pure nonpolar (10 $\bar{1}$ 0)_{ZnO}, whereas it is in semipolar (11 $\bar{2}$ $\bar{2}$)_{ZnO} on the oxygen-annealed LAO. As the ZnO films were deposited in the same condition, the growth difference may be associated with the

* Corresponding author. Tel.: +886 3 573 1615, fax: +886 3 572 4727.
E-mail address: lichang@cc.nctu.edu.tw (L. Chang).

interface between ZnO and LAO. Thus, the annealing effect of (112) LAO on the epitaxial relationship of ZnO is further investigated by inspecting their interface structures.

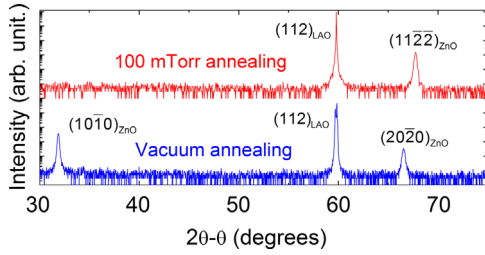


Fig. 1. XRD 2θ - θ scans of ZnO grown on (112) LAO substrates with different annealing conditions prior to ZnO deposition.

Fig. 2 shows HAADF images viewed along $[1\bar{1}0]_{\text{LAO}}$ zone axis near the interface of ZnO/LAO. The brightest spots in the bottom half indicate La–O atomic columns, and the less bright spots in the top half are of Zn and O in superposition along $[1\bar{1}0]_{\text{LAO}}$. From Fig. 2(a) and (b), it can be derived that the epitaxial relationships of $(10\bar{1}0)_{\text{ZnO}}$ and $(11\bar{2}\bar{2})_{\text{ZnO}}$ with LAO substrates are $[0001]_{\text{ZnO}}//[\bar{1}\bar{1}0]_{\text{LAO}}$ and $[1\bar{1}00]_{\text{ZnO}}//[\bar{1}\bar{1}0]_{\text{LAO}}$, respectively. Besides, it shows that the interface of $(10\bar{1}0)_{\text{ZnO}}/(112)_{\text{LAO}}$ is smooth, and the interface of $(11\bar{2}\bar{2})_{\text{ZnO}}/(112)_{\text{LAO}}$ is slightly rough. Fig. 2(c) and (d) in enlarged view clearly reveal that the $(10\bar{1}0)_{\text{ZnO}}$ lattices connect very well with LAO ones at the atomic flat $(112)_{\text{LAO}}$ interfacial plane, and $(11\bar{2}\bar{2})_{\text{ZnO}}$ is mainly on the LAO surface with $(001)_{\text{LAO}}$ and $(110)_{\text{LAO}}$ facets in atomic scale. This suggests that the LAO surface exhibits flat $(112)_{\text{LAO}}$ planes after vacuum annealing, but it can be decomposed into $(001)_{\text{LAO}}$ and $(110)_{\text{LAO}}$ facets in atomic scale after annealing in oxygen.

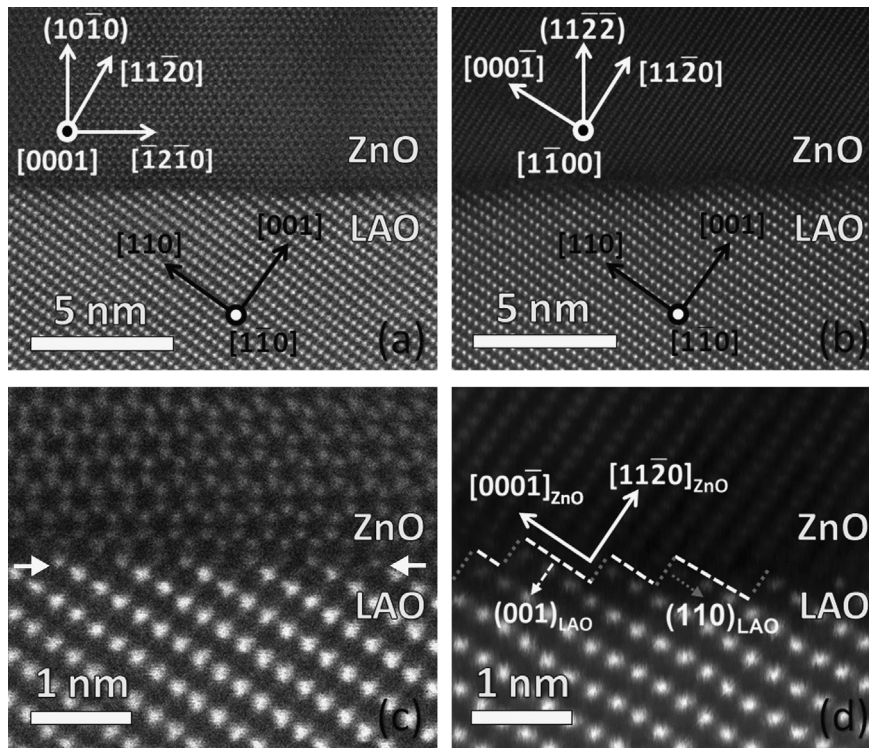


Fig. 2. (a) and (b) High-resolution STEM HAADF images of $(10\bar{1}0)$ and $(11\bar{2}\bar{2})_{\text{ZnO}}$ on (112) LAO viewed along $[1\bar{1}0]_{\text{LAO}}$, respectively. (c) and (d) Enlarged HAADF images of (a) and (b), respectively. The arrows and dash lines in (c) and (d) indicate the interfaces, respectively.

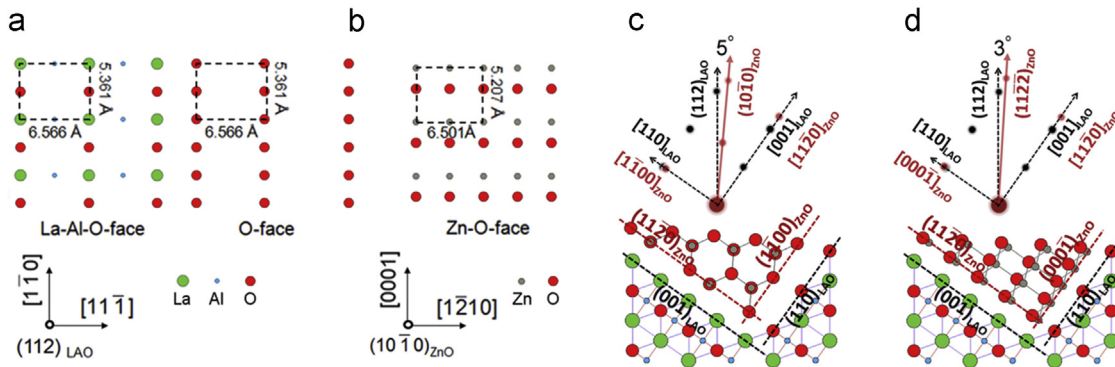


Fig. 3. (a) and (b) Atomic configurations of (112) LAO and $(10\bar{1}0)_{\text{ZnO}}$, respectively. They are arranged according to their epitaxial relationships. The dash lines represent in-plane unit cells in each plane. (c) and (d) Orientation relationships of ZnO on (112) LAO with $(11\bar{2}\bar{2})_{\text{ZnO}}$ planes parallel to $(001)_{\text{LAO}}$ facets viewed along $[0001]_{\text{ZnO}}//[\bar{1}\bar{1}0]_{\text{LAO}}$ and $[1\bar{1}00]_{\text{ZnO}}//[\bar{1}\bar{1}0]_{\text{LAO}}$, respectively.

The atomic configurations of ZnO on (112) LAO are schematically drawn in Fig. 3 for (10–10) ZnO on flat (112) LAO and (11 $\bar{2}$ $\bar{2}$) ZnO on the faceted (112) LAO. In Fig. 3(a), there are two kinds of terminations of (112)_{LAO} planes, La–Al–O-face and O-face, while only one termination of (10 $\bar{1}0$)_{ZnO} planes in Fig. 3(b). The (10 $\bar{1}0$)_{ZnO} plane shows cation and anion rows alternating along $\langle 0001 \rangle_{\text{ZnO}}$ and is similar to the atomic arrangement of La–Al–O-face, whereas the O-face of (112) LAO is terminated with anions only. Therefore, the cation (or anion) rows of (10 $\bar{1}0$)_{ZnO} would like to match the opposite-charged rows of La–Al–O face of (112) LAO to minimize the Coulomb potential at the interface. Furthermore, their lattice mismatch along [0001]_{ZnO} and [1 $\bar{2}$ 10]_{ZnO} is only +2.9% and +1%, respectively. Thus, these features can account for why the (10 $\bar{1}0$) ZnO forms on flat (112)_{LAO}.

For semipolar (11 $\bar{2}$ $\bar{2}$) ZnO grown on the faceted surface of (112) LAO, ZnO would first form at the steps of adjacent facets where deposited species can arrive through effective migration on substrate surface allowed by the deposition condition at 750 °C, followed by subsequent growth. Therefore, the growth of ZnO may be affected by both (001)_{LAO} and (110)_{LAO} facets. For the ZnO on (001)_{LAO} plane, the growth relationship can be similar to that reported for the growth of (11 $\bar{2}0$) ZnO on (001) LAO with [0001]_{ZnO}//[1 $\bar{1}0$]_{LAO} and [1 $\bar{1}00$]_{ZnO}//[1 $\bar{1}0$]_{LAO} [8]. Thus, the orientation relationship of ZnO on faceted (112) LAO can be illustrated with (11 $\bar{2}0$) ZnO on (001)_{LAO} facets as shown in Fig. 3(c) and (d).

Among various possible interface models, Fig. 3(c) and (d) are the more realistic ones in which terminations of (001)_{LAO} and (110)_{LAO} facets are determined by comparing the positions of adjacent Zn and La columns in Fig. 2(d). In Fig. 3(c), ZnO with the relationship of [0001]_{ZnO}//[1 $\bar{1}0$]_{LAO} shows (10 $\bar{1}0$)_{ZnO} plane having an inclination of 5° to (112) LAO, whereas ZnO with the relationship of [1 $\bar{1}00$]_{ZnO}//[1 $\bar{1}0$]_{LAO} in Fig. 3(d) shows (11 $\bar{2}$ $\bar{2}$)_{ZnO} plane in an inclination of 3° to (112) LAO. The orientation relationships in Fig. 3(c) and (d) are similar to the observations in Fig. 2 (a) and (b), respectively. Therefore, both (10 $\bar{1}0$) and (11 $\bar{2}$ $\bar{2}$) ZnO could form on the faceted (112) LAO surface. However, only (11 $\bar{2}$ $\bar{2}$) ZnO has been observed on the faceted LAO surface, suggesting that (110)_{LAO} facets may also affect the formation of ZnO. The effect of (110)_{LAO} facets can be interpreted from the point of view that on (110)_{LAO} surface the growth of ZnO may be more favorable along polar $\langle 000\bar{1} \rangle_{\text{ZnO}}$ than nonpolar [1 $\bar{1}00$]_{ZnO}. In Fig. 3(c) and (d), both (110)_{LAO} and (000 $\bar{1}$)_{ZnO} planes show altering negative and positive electrical-charged layers, but nonpolar [1 $\bar{1}00$]_{ZnO} is electrically neutral. Due to the ionic characters of LAO and ZnO, the interface constituted by (000 $\bar{1}$)_{ZnO} and (110)_{LAO} layers with opposite electrical charge may be more energetically favorable than [1 $\bar{1}00$]_{ZnO}/(110)_{LAO} interface. In addition, a good match between (000 $\bar{1}$)_{ZnO} and (110)_{LAO} is also shown in Fig. 3(d) that at the interface the positions of Zn ions of (000 $\bar{1}$)_{ZnO} can be in good

alignment with those of La and Al ions next to the oxygen layer of (110)_{LAO} along [000 $\bar{1}$]_{ZnO}. Further, we can obtain the growth of the c-plane ZnO on (110) LAO substrates in the same annealing and deposition conditions for LAO and ZnO with the epitaxial relationship of [1 $\bar{1}00$]_{ZnO}//[1 $\bar{1}0$]_{LAO} (not shown here). Such a relationship of c-ZnO on (110) LAO is coincident with that shown in Fig. 3(d), implying that the ZnO/LAO interface should accommodate appropriate match with not only (001)_{LAO} but also (110)_{LAO} facets on (112) LAO. As a result, the oriented ZnO growth on the faceted (112) LAO surface leads to the epitaxial growth of (11 $\bar{2}$ $\bar{2}$) ZnO films.

4. Conclusions

We have shown that the growth of ZnO on (112) LAO substrates can be varied to form nonpolar and semipolar orientations by adjusting annealing conditions of LAO with and without oxygen, respectively. The growth of (10 $\bar{1}0$) ZnO is achieved on flat (112) LAO surface due to small lattice mismatch, while (11 $\bar{2}$ $\bar{2}$) ZnO can be resulted from the growth of (11 $\bar{2}0$) ZnO on (001)_{LAO} facets and (000 $\bar{1}$) ZnO on (110)_{LAO} facets with [1 $\bar{1}00$]_{ZnO}//[1 $\bar{1}0$]_{LAO}.

Acknowledgments

This work was supported by the National Science Council, Taiwan (Contract no. NSC98-2221-E-009-042-MY3).

References

- [1] Makino T, Chia CH, Tuan NT, Sun HD, Segawa Y, Kawasaki M, et al. Appl Phys Lett 2000;77:975–7.
- [2] Takeuchi T, Sota S, Katsuragawa M, Komori M, Takeuchi H, Amano H, et al. Jpn J Appl Phys 1997;36:L382–5.
- [3] Kim MH, Schubert MF, Dai Q, Kim JK, Schubert EF, Piprek J, et al. Appl Phys Lett 2007;91:183507.
- [4] Speck JS, Chichibu SF. MRS Bull 2009;34:304–12.
- [5] Masui H, Nakamura S, DenBaars SP, Mishra UK. IEEE Trans Electron Dev 2010;57:88–100.
- [6] Gorla CR, Emanetoglu NW, Liang S, Mayo WE, Lu Y, Wraback M, et al. J Appl Phys 1999;85:2595–602.
- [7] Ho YT, Wang WL, Peng CY, Liang MH, Tian JS, Lin CW, et al. Appl Phys Lett 2008;93:121911.
- [8] Moriyama T, Fujita S. Jpn J Appl Phys 2005;44:7919–21.
- [9] Chou MMC, Chang L, Chung HY, Huang TH, Wu JJ, Chen CW. J Cryst Growth 2007;308:412–6.
- [10] Ho YH, Wang WL, Peng CY, Chen WC, Liang MH, Tian JS, et al. Phys Status Solidi RRL 2009;3:109–11.
- [11] Ho YT, Wang WL, Peng CY, Tian JS, Shih YS, Yen TC, et al. Phys Status Solidi RRL 2012;6:114–6.
- [12] Tian JS, Peng CY, Wang WL, Wu YH, Shih YS, Chiu KA, et al. Phys Status Solidi RRL 2013;7:293–6.